

Received February 7, 2020, accepted February 24, 2020, date of publication March 11, 2020, date of current version March 20, 2020.

Digital Object Identifier 10.1109/ACCESS.2020.2980057

Quasi-Global Optimization of Antenna Structures Using Principal Components and Affine Subspace-Spanned Surrogates

JON ATLI TOMASSON¹, SLAWOMIR KOZIEL^{1,2}, (Senior Member, IEEE),
AND ANNA PIETRENKO-DABROWSKA², (Member, IEEE)

¹Engineering Optimization and Modeling Center, Reykjavik University, Reykjavik 101, Iceland

²Faculty of Electronics, Telecommunications and Informatics, Gdansk University of Technology, 80-233 Gdansk, Poland

Corresponding author: Anna Pietrenko-Dabrowska (anna.dabrowska@pg.edu.pl)

This work was supported in part by the Icelandic Centre for Research (RANNIS) under Grant 174573051, and in part by the National Science Centre of Poland under Grant 2017/27/B/ST7/00563.

ABSTRACT Parametric optimization is a mandatory step in the design of contemporary antenna structures. Conceptual development can only provide rough initial designs that have to be further tuned, often extensively. Given the topological complexity of modern antennas, the design closure necessarily involves full-wave electromagnetic (EM) simulations and—in many cases—global search procedures. Both factors make antenna optimization a computationally expensive endeavor: population-based metaheuristics, routinely used in this context, entail significant computational overhead. This letter proposes a novel approach that interleaves trust-region gradient search with iterative parameter space exploration by means of local kriging surrogate models. Dictated by efficiency, the latter are rendered in low-dimensional subspaces spanned by the principal components of the antenna response Jacobian matrix, extracted to identify the directions of the maximum (frequency-averaged) response variability. The aforementioned combination of techniques enables quasi-global search at the cost comparable to local optimization. These features are demonstrated using two antenna examples as well as benchmarking against multiple-start local tuning.

INDEX TERMS Antenna optimization, EM-driven design, gradient-based search, principal component analysis, kriging

I. INTRODUCTION

Development of modern antennas necessarily involves parameter tuning, typically being the last stage of the design process. For reliability, it is executed at the level of full-wave electromagnetic (EM) simulation models. This is to capture the effects and phenomena (mutual coupling [1], the presence of connectors and housing [2], feed radiation [3], etc.) that affect the antenna performance but cannot be accounted for using simpler methods, e.g., analytical or equivalent network models. Although imperative, EM-driven design may entail considerable computational expenses. In situations where reasonably good initial design is not available or the problem is heavily multimodal [4], local optimization is insufficient and executing global search might be unavoidable. Examples include pattern synthesis of antenna arrays [5],

design of compact antennas [6], or cases that require handling of multiple objectives and constraints (circularly polarized antennas [7], MIMO systems [8]).

Conventional approaches to global optimization are largely based on population-based metaheuristics, where the exchange of information between the search agents enables comprehensive exploration of the design space and escaping from local optima [9]. Popular techniques include evolutionary algorithms [10], particle swarm optimizers [11], differential evolution [12], harmony search [13], and many other methods [14]–[16], essentially being slight variations of the popular routines. Due to tremendous computational cost of metaheuristics, direct handling of EM simulation models is often prohibitive. One way of alleviating this difficulty are machine learning approaches involving iterative construction of fast surrogate models [17], [18]. These are typically associated with sequential sampling [19], where the current surrogate, constructed from available EM simulation data, is used

The associate editor coordinating the review of this manuscript and approving it for publication was Mohammed Bait-Suwailam¹.

to identify the promising regions of the parameter space as well as to allocate the infill samples, subsequently used to update the model [19]. Other available techniques include multiple-start local optimization, the Taguchi method involving experimental design by orthogonal arrays [20], as well as combinations of metaheuristics with gradient-based procedures (e.g., [21]) or variable-fidelity simulations (e.g., [22]), both incorporated to speed up the convergence process. Yet, these alternatives have gained limited popularity. Despite their deficiencies, metaheuristics remain the dominant algorithmic solutions in the context of global optimization.

This letter proposes a novel approach to quasi-global optimization of antenna structures. Our methodology combines the trust-region gradient search with the parameter space exploration realized using local kriging metamodels. The surrogates are iteratively constructed within low-dimensional subspaces spanned by the principal components of the antenna response gradients. The latter are set up to identify the directions corresponding to the maximum (frequency-averaged) variability of antenna characteristics, which enables traversing the design space at a low cost. This idea has been adopted from [23], where the principal component analysis (PCA) was used in the context of local search, specifically, to identify directions subjected to finite-differentiation updates of the Jacobian matrix. Interleaving the trust-region algorithm and surrogate-assisted exploration results in quasi-global search capabilities while maintaining computational efficiency of the process. This is comprehensively demonstrated using two antenna examples. At the same time, benchmarking against multiple-start local optimization corroborates the robustness of the proposed method.

II. QUASI-GLOBAL OPTIMIZATION BY PCA AND METAMODELS

This section describes the proposed design optimization framework. We start by highlighting the overall concept, followed by the algorithm flow as well as detailed explanations of the key components of the procedure. Demonstration examples can be found in Section III.

A. DESIGN CLOSURE PROBLEM FORMULATION

Let $\mathbf{R}(\mathbf{x})$ stand for the output of the EM simulation model of the antenna under design (e.g., reflection or gain versus frequency) with $\mathbf{x} = [x_1 \dots x_n]^T \in X$ being a vector of adjustable variables. Typically, the parameter space X is defined by the lower and upper bounds $\mathbf{l} = [l_1 \dots l_n]^T$ and $\mathbf{u} = [u_1 \dots u_n]^T$ so that $l_k \leq x_k \leq u_k, k = 1, \dots, n$. Given the scalar merit function U quantifying the design utility, the optimization task can be defined as

$$\mathbf{x}^* = \arg \min_{\mathbf{x} \in X} U(\mathbf{R}(\mathbf{x})) \quad (1)$$

A representative example is optimization for minimum reflection over a specified frequency range F , where the merit function can be defined as $U(\mathbf{R}(\mathbf{x})) = U(S_{11}(\mathbf{x}, f)) = \max\{f \in F: |S_{11}(\mathbf{x}, f)|\}$. This makes (1) a minimax problem.

B. ALGORITHM FLOW

The goal of the optimization framework is to enable a quasi-global search while maintaining low computational complexity. A prerequisite is an implementation of some sort of parameter space exploration. Here, low cost of the process is ensured by predominantly employing local search mechanisms as well as restricting the space dimensionality at the exploration stages.

The operation of the proposed algorithm is outlined below, whereas the details concerning its most important components are provided in Sections II.B through II.D (here, N_0 , N_1 , and N_{\max} are the control parameters, whereas $\text{card}(Y)$ stands for the cardinality of the set Y):

1. Uniformly allocate N_0 random samples $\mathbf{x}_j^{(k)} \in X$;
2. Assign $\mathbf{x}^{(0)} = \min\{k = 1, \dots, N_0: U(\mathbf{R}(\mathbf{x}_j^{(k)}))\}$;
3. Set the iteration index $i = 0$;
4. Evaluate Jacobian $\mathbf{J}_R(\mathbf{x}^{(i)})$;
5. Use $\mathbf{J}_R(\mathbf{x}^{(i)})$ to identify the subspace $S^{(i)}$ of maximum antenna response variability (cf. Section II.C);
6. Allocate N_1 samples $\mathbf{x}^{(i,k)}, k = 1, \dots, N_1$, within $S^{(i)} \cap X$;
7. Build kriging surrogate $\mathbf{R}_s^{(i)}$ therein using $\{\mathbf{x}^{(i,k)}, \mathbf{R}(\mathbf{x}^{(i,k)})\}$ as the training set (cf. Section II.D);
8. Find the candidate design \mathbf{x}_{mp} by (globally) optimizing the surrogate $\mathbf{R}_s^{(i)}$:

$$\mathbf{x}_{mp} = \arg \min_{\mathbf{x} \in S^{(i)} \cap X} U(\mathbf{R}_s^{(i)}(\mathbf{x})) \quad (2)$$

9. Starting from \mathbf{x}_{mp} , find the new design $\mathbf{x}^{(i+1)}$ through local optimization of the EM model \mathbf{R} (cf. Section II.E)

$$\mathbf{x}^{(i+1)} = \arg \min_{\mathbf{x} \in X} U(\mathbf{R}(\mathbf{x})) \quad (3)$$

10. **If** $U(\mathbf{R}(\mathbf{x}^{(i+1)})) < U(\mathbf{R}(\mathbf{x}^{(i)}))$ then
 Accept $\mathbf{x}^{(i+1)}$ and set $i = i + 1$;
 else
 If $\text{card}(\{\mathbf{x}^{(i,k)}\}) \leq N_{\max}$
 Allocate N_2 additional (infill) samples within $S^{(i)} \cap X$; go to 7;
 else
 Return $\mathbf{x}^* = \mathbf{x}^{(i)}$.
 end
 end
11. **If** the termination condition is not satisfied, go to 4;
 else return $\mathbf{x}^* = \mathbf{x}^{(i)}$.

The algorithm starts by rough exploration of the parameter space and initialization of the main algorithm from the best point $\mathbf{x}^{(0)}$ found at that stage of the process. Each iteration consists of establishing the subspace $S^{(i)}$ spanned by the principal components of the Jacobian matrix, calculated to determine the directions of the maximum antenna response variability (Steps 4 and 5). The subspace is of low dimension (typically, two), which permits a construction of reliable surrogate in $S^{(i)} \cap X$ using a small number of samples N_1 (Steps 6 and 7). The surrogate is subsequently used as a predictor to identify the best design within $S^{(i)} \cap X$

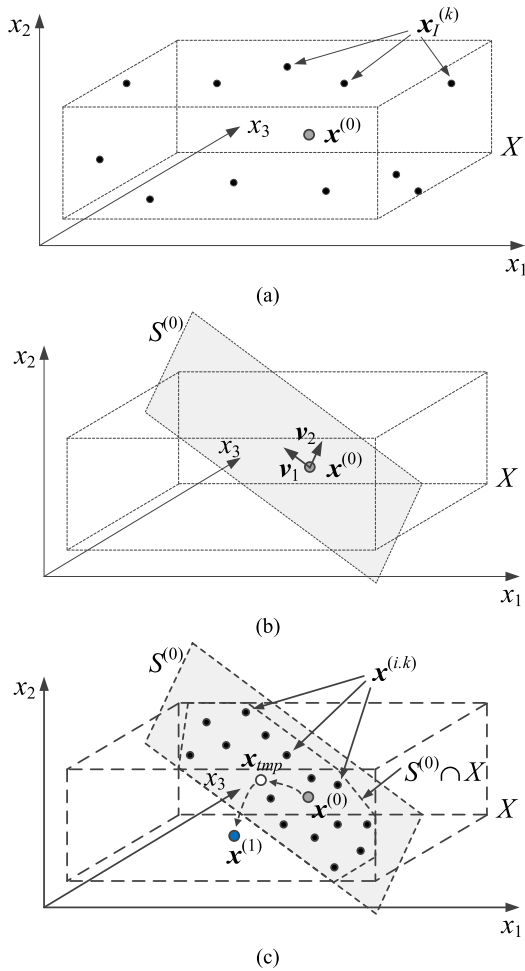


FIGURE 1. Basic steps of the proposed quasi-global optimization procedure (illustrated for a three-dimensional case): (a) parameter space X , initial sampling, and the best design $x^{(0)}$ over the sample set (Steps 1 and 2), (b) first iteration: subspace $S^{(0)}$ spanned by the first two principal directions (Steps 4 and 5), (c) sampling of $S^{(0)} \cap X$ (Step 6), construction of the surrogate (Step 7), subsequently optimized to find x_{tmp} (Step 8), and the follow-up gradient-based refinement yielding the next design $x^{(1)}$ (Step 9).

(Step 8) which is followed by low-cost EM-driven local optimization (Step 9). Upon finding a better design, the iteration is repeated. In the case of failure, the surrogate model is refined by adding infill samples (Step 10). The termination condition is based on the maximum computational budget and the convergence in argument. Figure 1 provides a graphical illustration of the essential algorithm stages. Note that Steps 1 and 2 can be replaced by employing a user-supplied initial design.

C. PRINCIPAL COMPONENTS AND SUBSPACE DEFINITION

Given the current design $x^{(i)}$, the goal is to define the directions corresponding to the maximum variability of the antenna responses using the Jacobian matrix $J_R(x^{(i)})$. If $R(x^{(i)})$ represents a frequency characteristic (e.g., antenna reflection) over a discrete set of frequencies $f_k, k = 1, \dots, m$,

we have $R(x^{(i)}) = [R(x^{(i)}, f_1) \dots R(x^{(i)}, f_m)]^T$ and

$$J_R(x^{(i)}) = [\nabla_1(x^{(i)}) \dots \nabla_m(x^{(i)})]^T \quad (4)$$

where the gradients are

$$\nabla_k^T(x^{(i)}) = \left[\frac{\partial R(x^{(i)}, f_k)}{\partial x_1} \dots \frac{\partial R(x^{(i)}, f_k)}{\partial x_n} \right] \quad (5)$$

The vector $\nabla_k(x^{(i)})$ determines the direction of the maximum antenna response variability at the frequency f_k . Consider the set $\{\nabla_k(x^{(i)})\}_{k=1, \dots, m}$ and its covariance matrix $C = (m-1)^{-1} S^T S$, where $S = |J_R| - \mathbf{1}\mu^T$ is a mean-subtracted matrix with $|J_R|$ being a matrix of the gradient moduli, $\mu = [\mu_1 \dots \mu_m]^T$ being the means gradient moduli, and $\mathbf{1}$ being the $m \times 1$ vector of all ones. We have [23]

$$C = VEV^{-1} \quad (6)$$

where $V = [v_1 \dots v_n]$ is a matrix of eigenvectors and E is a diagonal matrix of the corresponding eigenvalues λ_i , here assumed to be arranged in a descending order $\lambda_1 \geq \dots \geq \lambda_n$. The eigenvalues represent the variances of the observable set $\{\nabla_k(x^{(i)})\}_{k=1, \dots, m}$ projected onto one-dimensional subspaces spanned by the corresponding eigenvectors. In other words, the eigenvectors v_k determine (in the descending order) the directions of the maximum antenna response variability averaged over the frequency range of interest.

The affine subspace $S^{(i)}$ of Step 5 of the optimization algorithm of Section II.B is then defined as

$$S^{(i)} = x^{(i)} + \sum_{j=1}^{N_s} a_j v_j \quad (7)$$

where a_j are real coefficients. In practice, we use $N_s = 2$ to facilitate the construction of the surrogate model and its optimization.

D. SURROGATE MODEL CONSTRUCTION

The surrogate model $R_s^{(i)}$ is constructed within $S^{(i)} \cap X$ using kriging interpolation [24]. The design of experiments is arranged using sequential sampling oriented towards the improvement of the model predictive power. The sampling flow is as follows:

1. Allocate the initial set of N_{init} training samples $x_t^{(k)}$ using Latin Hypercube Sampling [25];
2. If $\text{card}(\{x_t^{(k)}\}) < N_1$, find a new sample that maximizes the mean square error (MSE) [26] of the current surrogate and add it to the training data set.

MSE maximization is carried out in the global sense; however, it is an inexpensive process due to low dimensionality of $S^{(i)}$. The surrogate optimization (2) (Step 8 of the algorithm) is also performed globally. In practice, it is arranged as the exhaustive search over the dense structured grid superimposed on $S^{(i)} \cap X$, followed by a local (gradient-based) refinement. The computational cost of this process is negligible because $R_s^{(i)}$ is fast and the dimensionality of $S^{(i)}$ is low.

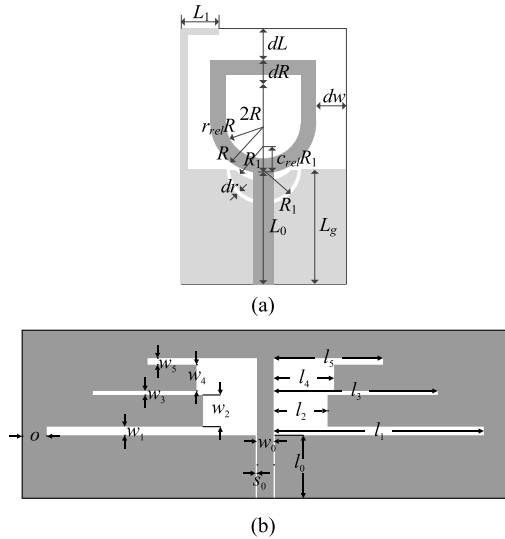


FIGURE 2. Geometries of the benchmark antennas: (a) wideband monopole [29] (ground plane shown using light-shade gray), (b) triple-band uniplanar dipole [30].

E. LOCAL OPTIMIZATION

A local design refinement of Step 9 of the algorithm of Section II.B is realized using the trust-region gradient-based algorithm yielding a series of approximations $\mathbf{x}^{(i+1,j)}$ to $\mathbf{x}^{(i+1)}$ as [27]

$$\mathbf{x}^{(i+1,j+1)} = \arg \min_{\mathbf{x}; -\mathbf{d}^{(j)} \leq \mathbf{x} - \mathbf{x}^{(i+1,j)} \leq \mathbf{d}^{(j)}} U(\mathbf{L}^{(j)}(\mathbf{x})) \quad (8)$$

where

$$\mathbf{L}^{(j)}(\mathbf{x}) = \mathbf{R}(\mathbf{x}^{(i+1,j)}) + \mathbf{J}_R(\mathbf{x}^{(i+1,j)}) \cdot (\mathbf{x} - \mathbf{x}^{(i+1,j)}) \quad (9)$$

The Jacobian matrix in (9) is estimated at $\mathbf{x}^{(i+1,0)} = \mathbf{x}_{imp}$ of (2) using finite differentiation, then updated using the rank-one Broyden formula [28] in subsequent iterations. This limits the cost of the algorithm (8) to one EM antenna simulation per iteration. The search process in (8) is restricted to the vicinity $\mathbf{x}^{(i+1,j)} - \mathbf{d}^{(j)} \leq \mathbf{x} \leq \mathbf{x}^{(i+1,j)} + \mathbf{d}^{(j)}$ of the current design, where $\mathbf{d}^{(j)}$ is the trust region size vector adaptively adjusted in each iteration [27].

III. DEMONSTRATION EXAMPLES

This section discusses validation of the proposed optimization strategy. We compare the result statistics obtained for several runs of the algorithm and the results of multiple-start gradient search. This is to verify the quasi-global search capabilities of the procedure. Our benchmark set includes a wideband monopole antenna and a triple-band uniplanar dipole.

A. CASE I: WIDEBAND MONOPOLE ANTENNA

The first test case is a wideband monopole antenna with quasi-circular radiator and a modified ground plane for bandwidth enhancement [29], see Fig. 2(a). The design variables are $\mathbf{x} = [L_0 \ dR \ Rr_{rel} \ dL \ dw \ L_g \ L_1 \ R_1 \ dr \ c_{rel}]^T$. The structure is implemented on Rogers RO4350 substrate ($\epsilon_r = 3.5$, $\tan\delta = 0.0027$, $h = 0.76$ mm). The computational model is implemented in CST Microwave Studio and evaluated using

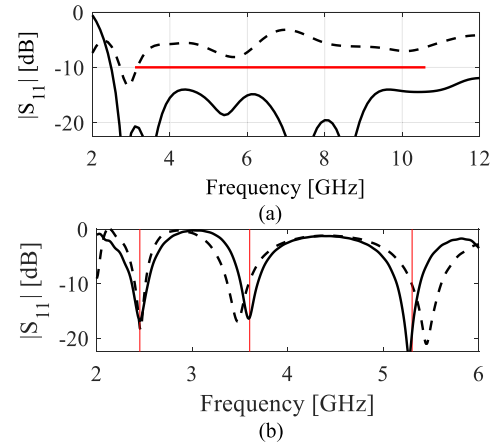


FIGURE 3. Reflection responses at $\mathbf{x}^{(0)}$ (- - -) and at the optimized design (-) for the selected runs of the proposed algorithm: (a) Wideband monopole, horizontal line indicates the design specifications. (b) Triple-band dipole, vertical lines indicate target operating frequencies.

TABLE 1. Optimization Results for Antennas I And II.

		Cost [#]	Success rate ^{##}	max S ₁₁ [§]	std max S ₁₁ [*]
Antenna I	Reference ^{&}	90.4	0.4	-6.6 dB	5.9 dB
	This work	287.1	1.0	-14.5 dB	1.5 dB
Antenna II	Reference ^{&}	99.4	0.25	-5.68 dB	4.9 dB
	This work	274.8	0.95	-13.5 dB	1.2 dB

[#] EM simulation count averaged over twenty algorithm runs with random initial points.

^{##} Proportion of runs where maximum |S₁₁| within frequency range was at least -10dB.

[§] Maximum |S₁₁| within frequency range averaged over twenty runs.

^{*} Standard deviation of max in-band gain in dB across the set of twenty algorithm runs.

[&] Standard trust-region gradient search algorithm with numerical algorithm, executed in 20 independent runs with random initial starting points.

its time-domain solver. The parameter space X is defined by the lower bounds $\mathbf{l} = [4.0 \ 0.0 \ 3.0 \ 0.1 \ 0.0 \ 0.0 \ 4.0 \ 0.0 \ 2.0 \ 0.2 \ 0.2]^T$ and the upper bounds $\mathbf{u} = [15.0 \ 6.0 \ 8.0 \ 0.9 \ 5.0 \ 8.0 \ 15.0 \ 6.0 \ 5.0 \ 1.0 \ 0.9]^T$. The design objective is to minimize |S₁₁| within the UWB frequency range of 3.1 GHz to 10.6 GHz. The control parameters N_0 , N_1 , and N_2 were set to 100, 50, and 10, respectively, for both verification cases.

The numerical experiments have been executed as follows:

- 20 runs of the proposed algorithm using new set of samples $\mathbf{x}_l^{(k)}$ for each run. The computational budget set to 300 EM simulations of the antenna;
- (benchmark) 20 runs of local search using the trust-region algorithm with numerical derivatives. Random initial points employed at each run.

Table 1 shows the result statistics. It can be observed that the proposed method yields satisfactory results in each run, whereas the success rate for the benchmark algorithm is only about forty percent. At the same time, the computational cost of the proposed procedure is practically acceptable: higher than local search but considerably less expensive than any conceivable population-based metaheuristic algorithm.

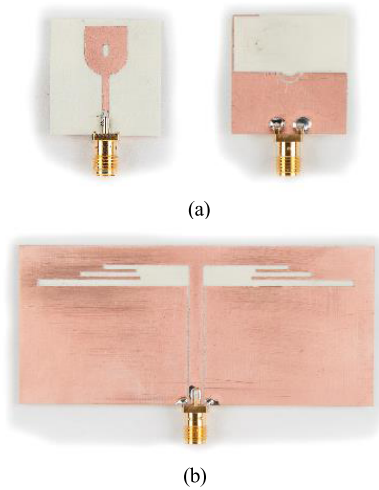


FIGURE 4. Photographs of the fabricated antenna prototypes: (a) wideband monopole, (b) triple-band dipole.

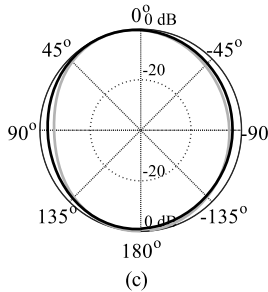
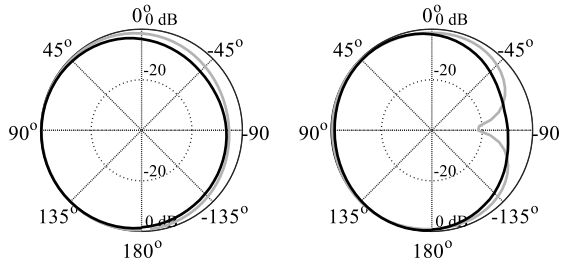
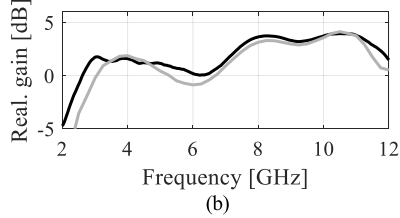
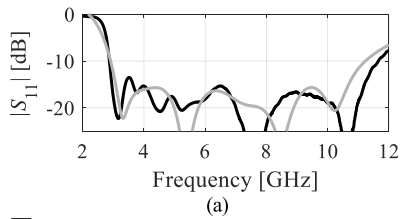


FIGURE 5. Wideband monopole: (a) reflection, (b) realized gain, (c) H-plane patterns at 4 GHz, 6 GHz, and 8 GHz; simulation (gray) and measurement (black).

Figure 3(a) shows the antenna reflection responses at the design $x^{(0)}$ (cf. Step 2, Section II.B) and upon optimization for a selected algorithm run.

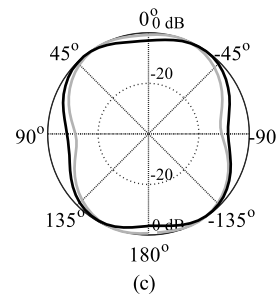
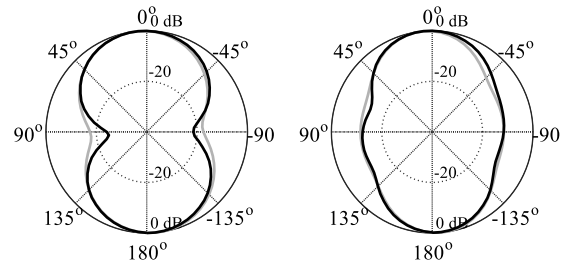
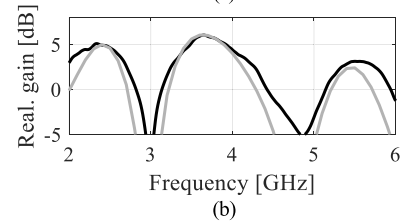
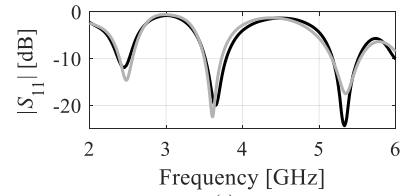


FIGURE 6. Triple-band dipole: (a) reflection, (b) realized gain, (c) H-plane patterns at 2.45 GHz, 3.6 GHz, and 5.3 GHz; simulation (gray) and measurement (black).

B. CASE II: UNIPLANAR DIPOLE ANTENNA

The second test case is a triple-band uniplanar dipole antenna shown in Fig. 2(b), based on the design of [30]. The structure is also implemented on RO4350 substrate, and fed through a 50 ohm coplanar waveguide (CPW).

The design variables are $x = [l_1 l_2 l_3 l_4 l_5 w_1 w_2 w_3 w_4 w_5]^T$; $l_0 = 30, w_0 = 3, s_0 = 0.15$ and $o = 5$ are fixed (all dimensions in mm). The parameter space X is defined by $l = [35 10 25 10 18 0.5 0.5 0.5 0.5 0.5]^T$ and $u = [40 15 30 15 22 2 1 1 1 1]^T$. Here, the goal is to minimize $|S_{11}|$ within the following bands: 2.4 GHz to 2.5 GHz, 3.55 GHz to 3.65 GHz, and 5.25 GHz to 5.35 GHz.

The experimental setup is the same as for the first test case. The numerical results are shown in Table 1. The results are consistent with those obtained for the first example. The proposed method yields satisfactory results in almost each run; the success rate for the benchmark algorithm is only about 25 percent, which demonstrates the need for global search. Figure 3(b) shows the reflection responses at $x^{(0)}$ and at the optimized design for a selected algorithm run.

C. DISCUSSION

The results reported in Section III.A and III.B indicate that the proposed algorithm dramatically improves reliability of the optimization process as compared to the local routines while retaining low computational cost of the process. The success rate is hundred percent for Antenna I and almost as much for Antenna II, which demonstrates the global search capability. Furthermore, the standard deviation of the final objective function values (last column of Table 1) is very small which confirms good repeatability of the results, i.e., robustness of the procedure.

D. EXPERIMENTAL VALIDATION

The selected optimized designs of both antennas have been fabricated and measured for additional validation. Figures 4 through 6 show the antenna prototypes as well as the reflection, realized gain, and radiation patterns. In both cases, the agreement between the simulated and measured data is satisfactory.

IV. CONCLUSION

This letter proposed a novel approach to quasi-global and computationally efficient design optimization of antenna structures. Our methodology combines surrogate-assisted space exploration and fast gradient-based local design refinement, integrated into an iterative procedure. To speed up the search process, the exploration stage is restricted to low-dimensional affine subspaces spanned by the directions corresponding to the maximum variability of antenna characteristics, extracted using principal component analysis. Comprehensive numerical validation demonstrates the efficacy of the method with satisfactory designs produced in almost each run of the algorithm and good result repeatability. This is in contrast to multiple-run local search the success rate of which is forty and twenty five percent for the two considered test cases, respectively. The additional advantages of the presented approach are algorithmic simplicity and low computational cost as compared to population-based metaheuristics.

REFERENCES

- [1] S. Kim and S. Nam, "A compact and wideband linear array antenna with low mutual coupling," *IEEE Trans. Antennas Propag.*, vol. 67, no. 8, pp. 5695–5699, Aug. 2019.
- [2] P. S. M. Yazeen, C. V. Vinisha, S. Vandana, M. Suprava, and R. U. Nair, "Electromagnetic performance analysis of graded dielectric inhomogeneous streamlined airborne radome," *IEEE Trans. Antennas Propag.*, vol. 65, no. 5, pp. 2718–2723, May 2017.
- [3] S. K. Karki, J. Ala-Laurinaho, V. Viikari, and R. Valkonen, "Effect of mutual coupling between feed elements on integrated lens antenna performance," *IET Microw., Antennas Propag.*, vol. 12, no. 10, pp. 1649–1655, Aug. 2018.
- [4] M. D. Gregory, Z. Bayraktar, and D. H. Werner, "Fast optimization of electromagnetic design problems using the covariance matrix adaptation evolutionary strategy," *IEEE Trans. Antennas Propag.*, vol. 59, no. 4, pp. 1275–1285, Apr. 2011.
- [5] S. Basbug, "Design and synthesis of antenna array with movable elements along semicircular paths," *IEEE Antennas Wireless Propag. Lett.*, vol. 16, pp. 3059–3062, 2017.
- [6] R. Bhattacharya, R. Garg, and T. K. Bhattacharyya, "Design of a PIFA-driven compact yagi-type pattern diversity antenna for handheld devices," *IEEE Antennas Wireless Propag. Lett.*, vol. 15, pp. 255–258, 2016.
- [7] U. Ullah and S. Koziel, "A broadband circularly polarized wide-slot antenna with a miniaturized footprint," *IEEE Ant. Wireless Prop. Lett.*, vol. 17, no. 12, pp. 2454–2458, Dec. 2018.
- [8] M. A. Fakhri, A. Diallo, P. Le Thuc, R. Staraj, O. Mourad, and E. A. Rachid, "Optimization of efficient dual band PIFA system for MIMO half-duplex 4G/LTE and full-duplex 5G communications," *IEEE Access*, vol. 7, pp. 128881–128895, 2019.
- [9] A. Deb, J. S. Roy, and B. Gupta, "A differential evolution performance comparison: Comparing how various differential evolution algorithms perform in designing microstrip antennas and arrays," *IEEE Antennas Propag. Mag.*, vol. 60, no. 1, pp. 51–61, Feb. 2018.
- [10] D. Ding and G. Wang, "Modified multiobjective evolutionary algorithm based on decomposition for antenna design," *IEEE Trans. Antennas Propag.*, vol. 61, no. 10, pp. 5301–5307, Oct. 2013.
- [11] A. Lalbakhsh, M. U. Afzal, and K. P. Esselle, "Multiobjective particle swarm optimization to design a time-delay equalizer metasurface for an electromagnetic band-gap resonator antenna," *IEEE Antennas Wireless Propag. Lett.*, vol. 16, pp. 912–915, 2017.
- [12] S. K. Goudos, K. Siakavara, T. Samaras, E. E. Vafiadis, and J. N. Sahalos, "Self-adaptive differential evolution applied to real-valued antenna and microwave design problems," *IEEE Trans. Antennas Propag.*, vol. 59, no. 4, pp. 1286–1298, Apr. 2011.
- [13] R.-Q. Wang and Y.-C. Jiao, "Synthesis of wideband rotationally symmetric sparse circular arrays with multiple constraints," *IEEE Antennas Wireless Propag. Lett.*, vol. 18, no. 5, pp. 821–825, May 2019.
- [14] A. Darvish and A. Ebrahimzadeh, "Improved fruit-fly optimization algorithm and its applications in antenna arrays synthesis," *IEEE Trans. Antennas Propag.*, vol. 66, no. 4, pp. 1756–1766, Apr. 2018.
- [15] A. Aldhfeeri and Y. Rahmat-Samii, "Brain storm optimization for electromagnetic applications: Continuous and discrete," *IEEE Trans. Antennas Propag.*, vol. 67, no. 4, pp. 2710–2722, Apr. 2019.
- [16] S. Karimkashi and A. A. Kishk, "Invasive weed optimization and its features in electromagnetics," *IEEE Trans. Antennas Propag.*, vol. 58, no. 4, pp. 1269–1278, Apr. 2010.
- [17] A. M. Alzahed, S. M. Mikki, and Y. M. M. Antar, "Nonlinear mutual coupling compensation operator design using a novel electromagnetic machine learning paradigm," *IEEE Antennas Wireless Propag. Lett.*, vol. 18, no. 5, pp. 861–865, May 2019.
- [18] J. Tak, A. Kantemur, Y. Sharma, and H. Xin, "A 3-D-printed W-band slotted waveguide array antenna optimized using machine learning," *IEEE Antennas Wireless Propag. Lett.*, vol. 17, no. 11, pp. 2008–2012, Nov. 2018.
- [19] H. M. Torun and M. Swaminathan, "High-dimensional global optimization method for high-frequency electronic design," *IEEE Trans. Microw. Theory Techn.*, vol. 67, no. 6, pp. 2128–2142, Jun. 2019.
- [20] W.-C. Weng, F. Yang, and A. Z. Elsherbeni, "Linear antenna array synthesis using Taguchi's method: A novel optimization technique in electromagnetics," *IEEE Trans. Antennas Propag.*, vol. 55, no. 3, pp. 723–730, Mar. 2007.
- [21] J. B. Liu, Z. X. Shen, and Y. L. Lu, "Optimal antenna design with QPSO-QN optimization strategy," *IEEE Trans. Magn.*, vol. 50, no. 2, Feb. 2014, Art. no. 7015904.
- [22] M. F. Pantoja, P. Meincke, and A. R. Bretones, "A hybrid genetic-algorithm space-mapping tool for the optimization of antennas," *IEEE Trans. Antennas Propag.*, vol. 55, no. 3, pp. 777–781, Mar. 2007.
- [23] I. T. Jolliffe, *Principal Component Analysis*, 2nd ed. New York, NY, USA: Springer, 2002.
- [24] N. V. Queipo, R. T. Haftka, W. Shyy, T. Goel, R. Vaidynathan, and P. K. Tucker, "Surrogate based analysis and optimization," *Prog. Aerosp. Sci.*, vol. 41, no. 1, pp. 1–28, Jan. 2005.
- [25] B. Beachkofski and R. Grandhi, "Improved distributed hypercube sampling," in *Proc. Amer. Inst. Aeronaut. Astronaut. (AIAA)*, 2002, p. 1274.
- [26] A. I. J. Forrester and A. J. Keane, "Recent advances in surrogate-based optimization," *Prog. Aerosp. Sci.*, vol. 45, nos. 1–3, pp. 50–79, Jan.-Apr. 2009.
- [27] A. R. Conn, N. I. M. Gould, and P. L. Toint, *Trust Region Methods*. Philadelphia, PA, USA: MPS-SIAM Series on Optimization, 2000.
- [28] C. G. Broyden, "A class of methods for solving nonlinear simultaneous equations," *Math. Comput.*, vol. 19, no. 92, p. 577, 1965.
- [29] M. G. N. Alsath and M. Kanagasabai, "Compact UWB monopole antenna for automotive communications," *IEEE Trans. Antennas Propag.*, vol. 63, no. 9, pp. 4204–4208, Sep. 2015.
- [30] Y.-C. Chen, S.-Y. Chen, and P. Hsu, "Dual-band slot dipole antenna fed by a coplanar waveguide," in *Proc. IEEE Antennas Propag. Soc. Int. Symp.*, Jul. 2006, pp. 3589–3592.



JON ATLI TOMASSON is currently pursuing the B.Sc. degree in mechatronic engineering with the Department of Engineering, Reykjavik University, Iceland. His research interests include simulation-driven design, surrogate-based optimization, evolutionary computation, dynamical systems, and stochastic processes.



SLAWOMIR KOZIEL (Senior Member, IEEE) received the M.Sc. and Ph.D. degrees in electronic engineering from the Gdansk University of Technology, Poland, in 1995 and 2000, respectively, the M.Sc. degrees in theoretical physics and in mathematics, in 2000 and 2002, respectively, and the Ph.D. degree in mathematics from the University of Gdansk, Poland, in 2003. He is currently a Professor with the School of Science and Engineering, Reykjavik University, Iceland. His research interests include the CAD and modeling of microwave and antenna structures, simulation-driven design, surrogate-based optimization, space mapping, circuit theory, analog signal processing, evolutionary computation, and numerical analysis.



ANNA PIETRENKO-DABROWSKA (Member, IEEE) received the M.Sc. and Ph.D. degrees in electronic engineering from the Gdansk University of Technology, Poland, in 1998 and 2007, respectively. She is currently an Associate Professor with the Gdansk University of Technology. Her research interests include simulation-driven design, design optimization, control theory, the modeling of microwave and antenna structures, and numerical analysis.

...